Development of a prototype for the analysis of multiple responses of the autonomic nervous system

Development of a Prototype for the Analysis of Multiple Responses of the Autonomic Nervous System

Daniela Naranjo[a,b], Ruggero Cattaneo[c], Luca Mesin[a,*]

[a] *Mathematical Biology and Physiology, Department of Electronics and Telecommunications, Politecnico di Torino, Torino, Italy*
[b] *Electronics and Nanotechnology Research Department, Fundación Clínica Shaio, Bogotá, Colombia*
[c] *Department of Health Sciences, Universitá di L'Aquila, L'Aquila, Italy*

Abstract

The autonomic nervous system (ANS) drives different non-voluntary responses, which can be investigated by multiple sensors. We propose a modular hardware prototype for the noninvasive acquisition, processing and transmission of biological signals to analyze the ANS in synchrony with the video recording of the pupil. The implementation includes 1) two noninvasive sensors, a pulse oximeter and an electrodermal activity sensor, 2) a module able to collect the information and send it to the PC via USB and 3) a graphic user interface for visualization, synchronization and data saving. A series of experimental tests were performed to investigate the effect of different stimulations: light, dental occlusion, transcutaneous electrical nerve stimulation (TENS) and mental efforts. They indicate the reliability of the system and the importance of the joint detection of more signals for discriminating different states of the ANS. Specifically, heart rate, Galvanic response and pupil size were compared, showing some coherence in their oscillations and a different ability to discriminate between the stimulation conditions. Their joint detection is thus important for discriminating different states of the ANS.

Keywords: Pulse oximetry, Electrodermal Activity (EDA), Galvanic Skin Response (GSR), Pupillogram, Autonomous Nervous System (ANS), Transcutaneous Electrical Nerve Stimulation (TENS), Embedded systems.

*Corresponding Author: Luca Mesin, Dipartimento di Elettronica e Telecomunicazioni, Politecnico di Torino, Corso Duca degli Abruzzi, 24 - 10129 Torino - Italy; Email, luca.mesin@polito.it; Phone, +39 011.090.4085

1. Introduction

The autonomic nervous system (ANS) is the portion of the central nervous system that controls unconscious activities, such as visceral functions and homeostasis [1]. It is divided into two main branches, the sympathetic and the parasympathetic, the first promoting the activation of a physiological response and the other inhibiting it. The ANS is profoundly affected by emotions and somatosensory inputs and plays an important role in pain and stress modulation and perception.

Autonomic testing finds application in the clinical assessment of neurological disorders, particularly those affecting predominantly small nerve fibres [2]. Many studies have been devoted to the quantitative assessment of the ANS response, dating back to more than 3 decades [3][4][5]. However, most of the literature takes into account just one of the numerous physiological systems that are affected by the ANS in turn.

Very frequently the works that have dealt with ANS in different disorders related to its dysfunction have focused on cardio-circulatory parameters [6]. However, there are many other potential peripheral effects of ANS which could be deepened. For example, a physiological system related to the ANS can be investigated measuring skin conductance, reflecting the sweating of the sweat glands [7]. Moreover, pupil is strongly affected by the ANS [8]. The study of mydriasis and myosis (i.e., the dilation and contraction of pupil) is usually done in a different context (vestibular system). However, recent studies have indicated the possibility of characterizing the condition of the ANS in healthy or pathological conditions, by analyzing the nonlinear pupil oscillations [9][10][11][12][13][14]. Moreover, the study of pupillary dynamics was considered useful for evaluating the arousal state during mental effort due to cognitive tasks [15][16], in relation to the involvement of reward systems [17] and in the development of Human-Machine Interfaces [18]. Furthermore, it has been suggested that the use of different ANS parameters, including pupil size, may be useful for better characterizing and quantifying the emotional component linked to the autonomous response [19]. Moreover, further evidence was provided that pupil can be used to evaluate the state of emotional arousal as well as the generic activation of the ANS [20].

One of the limitations of the study of various ANS responses is the use of different instruments for the analysis of different signals. However, it was argued that pupillogram could provide useful information for the study of the arousal state and that it would receive a valid contribution from the

association with signals already used for this purpose, such as skin conductance and electrocortical activity [21]. These observations would involve an important expansion of the combined and synchronous study of various parameters associated with pupillography to aspects not only of pathology, but also related to the emotional / affective state. Thus, important outcomes could be expected both for clinical patients and for any study involving the psychic assessment of the arousal state.

Only recently, more reactions of the ANS have been investigated simultaneously [22][23]. The signals that have been often analyzed are the cardiac pulse and the variations of skin conductance. In this study, we are interested in the investigation of those signals jointly with the pupil response. A modular hardware prototype is developed for the noninvasive acquisition, processing and transmission of biological signals and is synchronized with a commercial system for pupil investigation. Our present implementation includes:

- two noninvasive sensors, a pulse oximeter and an electrodermal activity sensor (both often used in the study of the responses of ANS [24][25][26]);
- a module able to collect the information and send it to the PC via USB;
- a graphic user interface (GUI) for visualization and data saving.

Pulse oximetry and skin conductivity are acquired in synchrony with the video recording of the patient's dilation and constriction of the pupil (acquired by a commercial system [27]). The system was developed to keep low the production cost and energy consumption. It was tested in experiments from healthy subjects under different stimulations: light, dental occlusion, transcutaneous electrical nerve stimulation (TENS) and computational task.

2. Design and Implementation

The recording system is shown in Figure 1. Two sensors, described below, are developed and are used together with a commercial system for pupil investigation [27].

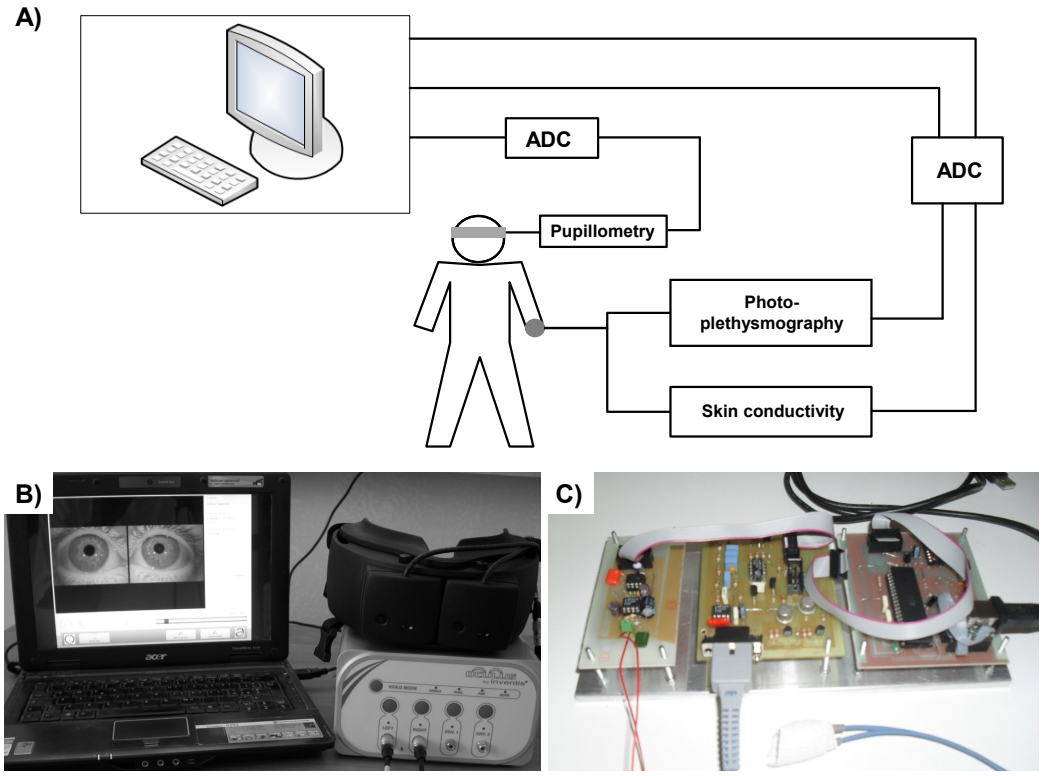

Figure 1: A) General scheme of the instrumentation used. B) Commercial system for pupil investigation [27]. C) Acquisition system recording photoplethysmogram and skin conductivity level.

2.1. Design of the sensors

2.1.1. Pulse oximeter.

The first sensor measures the absorption of red and infrared lights that pass through a patient's finger by light sensors. The light is generated with 2 LEDs that are controlled alternately. A photodiode receives both ambient and modulated light from the LED and generates a current that is related to the oxygen saturation and the cardiac frequency [28][29][30]. The pulse oximetry signal (photoplethysmogram - PPG) has an amplitude of aproximately 300 nA and a frequency range related to the heart rate (which is about 1 Hz), with maximum frequency contributions of a few Hz [31]. The signal is affected by the line interference (50 Hz), the neon lamps that are usually used in offices and laboratories (giving an interference at 100 Hz) and motion artifacts (notice that high performance professional oximeters are stable to ambient light and motion artifacts [32], but our low cost system had to rely on simple solutions). The circuit design is shown in Figure 2A and B. The current signal is transformed into a voltage signal in the 0.1 V-0.3 V range using a transimpedance amplifier with a gain of 820 kV/A. An initial bandpass filter with cut-off frequencies of 0.8 and 15 Hz was implemented; however powerline and neon lamps interferences were still visible in the resulting signal, therefore two notch filters were added to remove their contributions. A final active low-pass filter with a gain G = 30 V/V was added to make up for losses in amplitude through the filtering stages, resulting in a total gain of 5 MV/A. For the actual implementation, the sampling frequency of the PPG is 220 Hz. Notice that this sample rate is very high (e.g., 100 Hz is usually used in clinical settings, but 25 Hz was found to be sufficient to get a reliable estimation of the pulse rate variability [33]): thus, it could be decreased for saving energy or memory.

2.1.2. Skin conductivity level sensor.

There are two skin resistance responses due to the electrodermal activity (EDA): the tonic and the phasic levels. The tonic level is the absolute level of resistance at a given moment in the absence of a measurable phasic response and is referred to as Skin Conductance Level (SCL). The phasic level or Skin Conductance Response (SCR) is superimposed on the tonic level and corresponds to the response to stimuli. The sum of the tonic and phasic response is the Galvanic Skin Response (GSR).

The skin conductance is obtained by measuring the current flow through the skin in response to a constant applied voltage. The circuit design is

shown in Figure 2C. For bipolar recordings, 0.5 V is recommended [34]. For a resolution of 0.01 μS (the minimum variation of the SCR [35][36]), the minimum current to be amplified is of 5 nA. The maximum input current of the amplifier is 15 μA (related to the maximum SCR and SCL), therefore the transimpedance of the circuit must be of 333 kΩ. This circuit has two independent outputs that allow the analysis of each component separately (however, their combination, i.e., the GSR, was considered in our tests shown in the following). The sampling frequency is 170 Hz. Notice that this sample rate is far beyond the Nyquist limit (even if some literature has suggested even to further increase it to allow to apply more easily complex analysis or advanced smoothing procedures [37]), so that it could be decreased if needed (e.g., to save power consumption or memory storage).

Table 1 summarizes the data acquired, the filters used and their frequency ranges, and the adopted sampling frequencies.

Signal	**Filtered Frequency Range**	**Sampling Frequency**
Pulse oximeter	0.8 Hz - 15 Hz Using a band-pass filter and additional 50 Hz and 100 Hz notch filters	220 Hz
Skin Conductivity Level (SCL)	0 - 15 mHz Using a low-pass passive filter	170 Hz
Skin Conductivity Response (SCR)	10 mHz - 1 Hz Using a decoupling capacitor and an active low-pass filter	170 Hz

Table 1: Signals acquired, frequency range of the signals and sampling frequency.

2.2. Digital signal processing and transmission

The information coming from the analogue sensors was converted into digital form, acquired, pre-processed and transmitted via USB to a PC. The microcontroller Atmel ATmega 16 accomplished these tasks [38][39]. Such a microcontroller was chosen as it is cheap and it has a high speed, a small code size and an analog multiplier (which can be used to implement digital filters). The connection of the microcontroller to the system is shown in Figure 3. Notice that the internal 10-bit ADC was used for sampling the skin conductance, whereas an external 16 bits analog-to-digital converter (ADC) was included to sample the PPG (the considered external ADC is AD7715,

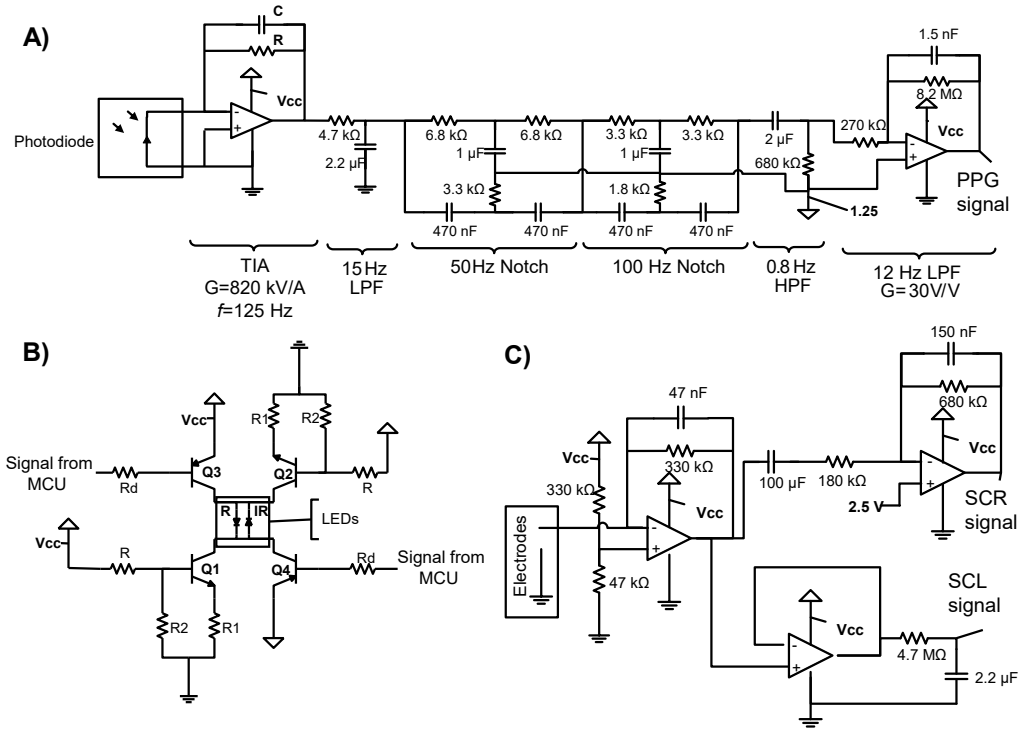

Figure 2: A) Schematic of the photoplethysmograph (abbreviations: PPG - photoplethysmogram; TIA - Transimpedance amplifier; LPF - low-pass filter; HPF - high-pass filter). B) Schematic of the LEDs driver. The signal from the microcontroller unit (MCU) controls which of the 2 LEDs is ON. C) Schematic of the skin conductance sensor. The 2 outputs are for the Skin Conductance Response (SCR) and the Skin Conductance Level (SCL).

which is a 16-bit Sigma-Delta ADC that can be interfaced with microcontrollers using the Serial Peripheral Interface, SPI). The ADC requires up to 195 μs for a single conversion, thus setting the sampling frequency of the signals once they have been converted to approximately 5 kHz. To remove noise added by the ADC, an average filter (of 5 samples for pulse oximetry and 20 samples for the Galvanic skin response) was implemented in the microcontroller. The filtered samples were then transmitted to the PC with the USART (Universal Synchronous/Asynchronous Receiver/Transmitter), which was interfaced with a USB transceiver.

The red and infrared lights for the pulse oximetry sensor must be ON in different cycles: the signal period was 1 ms, with a duty cycle of 0.25 and the phase between the two lights was 0.5 ms. The state of the LEDs was controlled using timer interrupt.

To manage the data, a software interface was developed in Visual Basic, with the following main functions.

- Registration of patient's information. The user should also be able to import the information from the database of pupillograms.
- Visualization of the signals. The charts update constantly to show the signals while they are being acquired.
- Storage of the signals. The information was stored in a file. This file contains the patient's information, the starting time of the acquisition (with a resolution of 10 ms), the time of each sample (recorded as lag from the starting time of acquisition) and the samples of the signals.

2.3. Pupillometry.

Images of the pupils were acquired by the Oculus system (Inventis srl, Padova, Italy), using two infrared CCD cameras (resolution 720x576 pixels, 256 grey levels) mounted on a light helmet (1.5 kg), with sampling frequency of 25 frame/s. The eyes were illuminated with an infrared diode with 880 nm of wave-length; moreover, during experiments on pupil dynamics under constant light conditions, illumination was provided by a yellow-green LED with 740 nm of wave-length.

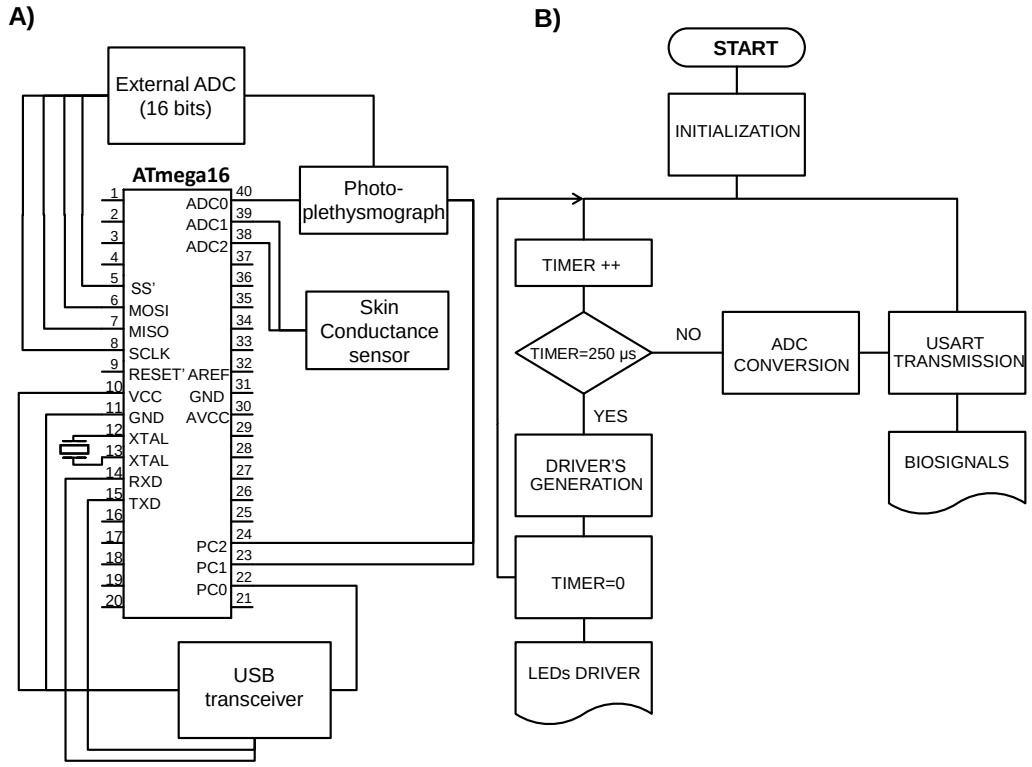

Figure 3: A) General schematic of the digital processing unit. B) Microcontroller general flow diagram.

3. Experimental tests

In order to assess the reliability of our acquisition system, a pilot study on a few healthy subjects was performed. Specifically, signals were acquired, synchronized and then processed, extracting some descriptors to characterize different experimental conditions.

3.1. Signal acquisition

Three signals were acquired and then synchronized for subsequent processing. Specifically, videos of the pupils were acquired by a commercial system (Section 2.3), whereas pulse oximetry and variations of sweat were monitored with the system described in the previous sections, considering the PPG and the GSR time series.

3.1.1. Synchronization of the signals.

The software of the considered system for pupil investigation [27] does not allow any kind of modifications or access. However, it allows to record the machine time in which each frame is acquired. The data from our prototype were recorded on the same PC. The starting time of the acquisition was saved (as mentioned above), with a resolution of 10 ms. Given that the sampling period of the pupillogram was 40 ms, this resolution was enough to synchronize the two systems.

3.1.2. Experimental set up.

The subjects were sitting in a high-back chair. The environment was kept at a constant temperature of 21^{o}C. Visual predominance was determined. The acquisition system was then connected to the patient's non dominant hand. The helmet was applied and was maintained until the end of the recording. This phase took about 4 minutes.

The correct procedure and execution of tests was first explained to the subjects. Then, they were asked for brief tests to make sure that the instructions were well understood. This phase took about 2 minutes.

Two operators worked within the experimental set. The first took care of the subject (pretest and test instructions, helmet handling, check of the correctness of execution), the second controlled hardware and software.

3.1.3. Experiments.

A few experimental tests were performed on 8 young and healthy subjects (age 25.1 ± 1.1 years; 6 females, 2 males). Small stimulations were administered to the participants, to test the ability of our prototype to register reliable data characterizing the response of the ANS. Specifically, stationary conditions of one minute duration which require a different involvement of the sympathetic and parasympathetic controls were considered, separated by 5 minutes rest. The following conditions were investigated: neutral position of the jaw (rest position: RP) and habitual dental occlusion (HDO)[1], in light or darkness condition; moreover, a test was performed during a computational task, which was assumed to induce a detectable stress of the subject. These 5 conditions (tested in the following order: RP in light and darkness, HDO in light and darkness and computational task in darkness) were performed before, during and after the application of low-frequency Transcutaneous Electrical Nerve Stimulation (TENS), which was expected to induce relaxation. TENS was applied as in previous studies [40], using a J5 Myomonitor TENS Unit device (Myotronics-Noromed, Inc., Tukwila, WA, USA) with disposable electrodes (Myotrode SG Electrodes, Myotronics-Noromed, Inc., Tukwila, WA, USA). Synchronous and bilateral stimuli, with amplitude adjusted in the range 0–24 mA and duration of 500 μs, have been delivered over the cutaneous projection of the notch of the fifth pair of cranial nerves (grounding electrode in the center of the back of the neck) at 0.66 Hz.

3.2. Signal processing and results

3.2.1. Pre-processing of recorded data.

Pupillometric recordings were processed through the algorithm of strongly connected components [41] to measure frame by frame the area of the pupil, expressed as the number of pixels covering it. The area of the pupil was then low-pass filtered under 2 Hz (non-causal, zero-phase, Butterworth filter of order 2). This frequency range is enough to characterize the response of the ANS of our interest, which mainly includes the following frequency ranges: low-frequency (LF) 0.04–0.15 Hz and high-frequency (HF) 0.15–0.5 Hz [9]. The local maxima in the PPG were used to identify the heartbeats, from

[1]During dental occlusion, the effect of muscle fatigue and the massive involvement of the autonomic system were excluded by avoiding prolonged teeth clenching. Subjects were asked to swallow and then to contact the teeth lightly without clenching. Attention was paid to check the activity of mimic muscles.

which the heart rate (HR) was estimated as the reciprocal of the inter-pulse interval.
The GSR was low-pass filtered under 2 Hz.

3.2.2. Estimation of indexes.

The following simple descriptors were estimated from the pre-processed data (pupillogram, i.e., pupil size over time), HR and GSR.

- The mean and standard deviation (STD) were computed to explore average values and variability, respectively.
- The linear trend was estimated as a basic indicator of the evolution in time of the signals (the trend was defined as the slope of the interpolation line of the data after scaling the time to range between 0 and 1 and normalizing the time series to have zero mean and unit STD).

3.2.3. Statistical analysis.

The indexes mentioned above were used as descriptors of the signals in the different experimental conditions. The two-sided Wilcoxon signed rank test (considering paired data) was then applied to investigate differences of each of the indexes in specific pairs of conditions of interest, after pooling data: RP in darkness compared to the computational task, RP compared to HDO (in darkness), pre-TENS compared to TENS or post-TENS conditions. The significance level was set to $p < 0.05$.

3.2.4. Results.

Examples of recorded signals are shown in Figure 4. The pupil shows an irregular oscillatory behavior, as also the HR. There is a decreasing trend in both HR and GSR. The figure shows also the spectral coherence of the pupillogram and the HR at frequencies lower than 1 Hz. The two signals were found to be coherent in subjects under controlled breathing conditions, where a respiratory component was visible in both the pupillogram and the HR [8]. Here, the considered normal breathing and the short acquisitions resulted in significant coherence (over 0.5) only in a few subjects and conditions.

The significance of the differences of indexes extracted from the signals recorded in different conditions is shown in Table 2. Different indexes have a greater discriminatory value comparing different conditions:

- an index from the HR showed the maximal significance (i.e., minimum p value) in discriminating computational task and RP in darkness (which can be considered as a rest state);

- indexes estimated from the pupillogram had the maximal significance in distinguishing light and darkness, RP and HDO, or pre-TENS and TENS conditions;

- indexes extracted from GSR were the most statistically different in the conditions pre-TENS versus post-TENS and TENS versus post-TENS.

Specifically, HR and mean pupil size increased when comparing computational task with RP in darkness (due to the mental stress induced by the task). The subject started sweating during the computational task, as indicated by the high positive trend of GSR. Pupil was the only system showing significant differences between HDO and RP: pupil size increased as a result of HDO stimulation [9][10][11]. Moreover, it was the only system showing significant differences comparing light and darkness conditions (obviously, increasing the diameter in darkness).

Pupil also indicated the relaxation induced by TENS (there is a significant reduction of pupil size during and after the application of TENS). On the other hand, GSR increased during and after TENS, with respect to the pre-TENS condition.

4. Discussion

The ANS controls many different visceral functions, including heart rate, perspiration, digestion, salivation, respiratory rate, pupillary dynamics, micturition (urination), sexual arousal, breathing and swallowing. The joint acquisition of different autonomic responses could be useful for a deeper insight into ANS physiology and pathology. For example, the study of the autonomic response is important in the following situations [42]:

- sympathetic and parasympathetic lesions after surgical procedures;

- drug's collateral effects;

- diagnosis and follow-up of ANS diseases;

- poisoning;

- involuntary reactions of the patient.

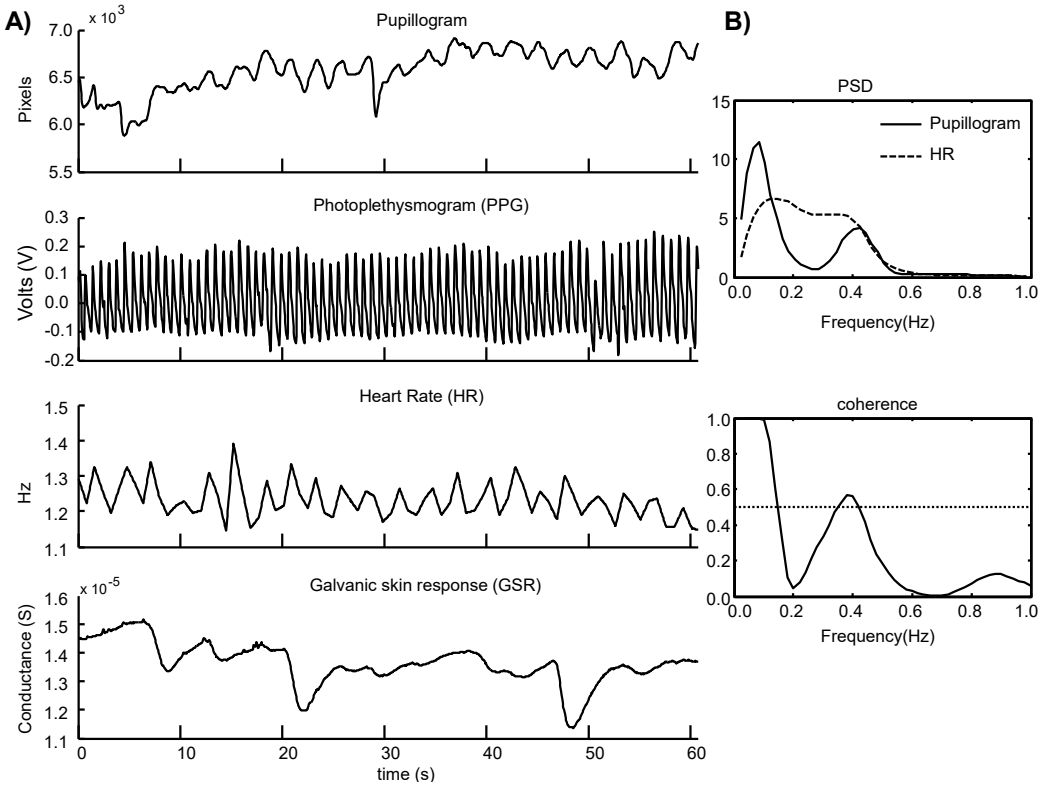

Figure 4: A) Example of data (pupillogram, PPG from which the HR is obtained, GSR), with the subject at rest position of the jaw in darkness. The HR was computed as the reciprocal of the inter-pulse interval. Each HR value was located in the average time between the two instants used to compute it, obtaining a time series (sampled not uniformly). Then, this time series, PPG and GRS were interpolated at 25 Hz (i.e., the sampling frequency of the pupillogram). B) Power spectrum densities (PSD) of pupillogram and HR (using Welch's overlapped segment averaging estimator, considering 8 segments with 50% overlap) and magnitude squared coherence.

The diagnosis in most of these situations is currently vague [43][44][45]. The joint investigation of different autonomic responses could help in clarifying the complex dynamics of the ANS in such conditions. One of the problems when designing an experimental setup is being constrained by the functionalities of commercial systems, which are usually closed and allow only specific protocols. Here, we were interested in investigating synchronously the joint responses of the heart (i.e., the cardiac pulse), the skin (i.e., sweat production) and pupil. Some devices have been developed for the joint acquisition of different ANS responses: both research prototypes [46][47][48] and commercial products (Q sensor, MOXO, Feel^{TM}, UP4, VIVOGRAPH, Microsoft Band, E4, Embrace) have been proposed. Despite the interest in the study of pupillary dynamics, at present there are no tools that are able to simultaneously obtain the acquisition and processing of pupillary dynamics and those of other systems such as the cardiovascular (e.g., through pulse oximetry) and sudorific system (through skin conductivity). Being able to expand the analysis to several systems in a synchronous way would allow a better knowledge of the coupling pathways between somatosensory and affective / emotional needs and responses of the whole of the ANS in physiological and/or pathological conditions, probably indicating the activation of different autonomous circuits in different conditions.

In this work, we have designed an experimental setup able to record in synchrony the video of pupil (done with a commercial system [27]) and different responses of the ANS. A modular sensor network was designed and implemented to acquire, process and transmit via USB some biomedical signals reflecting the state of the ANS. Two sensors have been included in the prototype, for pulse oximetry and skin conductivity. However, it is feasible for being extended to include more body sensors, miniaturized and embedded in a portable system. This could be important for future extension of the work, as body sensor networks are finding many applications in the continuous monitoring of sensitive people [49][50][51][52][53]. Indeed, many different sensors are available to monitor physiological data and could be included: accelerometer, blood glucose sensor, electrodes for bioelectric signals, blood pressure sensor, gyroscope, carbon dioxide gas sensor, etc. [53][54].
The developed system, even if it is only a prototype, provided robust estimations of the electrodermal activity and of the pulse oximetry, which was then processed to investigate the heart inter-beat interval. Note that the PPG is immune to electrical artifacts, which could be observed on the electrocardiogram during TENS application (however, it is less precise in detecting

the HR, as it also depends on the pulse wave velocity). Thus, our system is adequate for the study of the ANS response to TENS reflected in the HR.

Preliminary experimental tests are shown. Some trends have been observed. For example, both HR and GSR are decreasing during the experiment shown in Figure 4. This could reflect that the subject was relaxing, as the recordings were acquired in a rest condition (i.e., rest position of the jaw in darkness). Moreover, GSR slowly increased during the experiments, with the results that its mean value was larger during and after TENS, with respect to the pre-TENS condition, even if TENS should relax the participants (as indicated by variations in pupil size). Possibly, this trend of GSR was only due to an accumulation of sweat during the experiment, as the sensors were kept fixed for all its duration.

However, some consistent outcomes were also observed. Specifically, even if we considered only short recordings, weak ANS stimulations (dental occlusion, light, TENS and a computational task) in healthy subjects and we extracted simple indexes (mean, STD and trend), we have shown statistically significant variations of at least an index in each pair of conditions. This indicates that the overall information provided by the joint recordings, not just that of each individual signal, should be used for the discrimination of the ANS responses in the different considered conditions. The results are in line with our expectations: HDO and computation elicit the sympathetic response (which should result in HR and GSR increasing and pupil dilation), TENS induces relaxation (determining a decrease of HR, GSR and pupil size). The sensory amplitude TENS that we administered has been shown to induce the response of different branches of the ANS, as the salivary [55], the cardiovascular [56], the neuromuscular systems [57] and, in particular, the one that governs the static and dynamic dimension of the pupil [40]. The effects of the sensory trigeminal TENS stimulation are probably to be attributed to a central system that modulates the mechanisms of arousal and, therefore, the autonomous efferent response [58][59] (that was observed in this study).

Pupil appeared to be the most sensible system, as it reflected even the small stimuli given by HDO or TENS. HR showed significant variations only in a few conditions (e.g., mean HR was significantly increased only by the computation task). GSR showed an important trend during computation, but it was prone to accumulation effects.

Our study has some limitations: a few experiments have been conducted and all on healthy volunteers; only three signals have been included; our

system for the recording of PPG and GSR is a simple prototype, which is surely more delicate and less stable than engineered commercial products. However, it pointed out the importance of integrating information from different systems controlled by the ANS, in particular pupil (which was the most sensitive to weak stimulations). Further studies are then suggested, both to improve and extend our preliminary results. For example, other tests and advanced processing techniques could provide specific indications in physiology or pathology, in future joint acquisitions of different responses of the ANS. Additional measures to guarantee reproducibility of the tests need to be developed, such as careful preparation in order to stabilize hemodynamic parameters. Moreover, additional sensors or stimulation signals could be included in the proposed device, due to its modular architecture.

5. Conclusions

We discuss the implementation of a modular system for the acquisition of different signals reflecting the responses of the ANS to stimulations. The signals were synchronized to the pupillogram recorded by a commercial system, showing the joint variations of pupil size, Galvanic response and photoplethysmogram. Small stimulations were given to the participants and only considering all different recorded signals the different responses of the ANS could be discriminated. Thus, these preliminary results suggest the importance of recording jointly multiple data in order to better characterize autonomic responses.

References

[1] D. Glick, The autonomic nervous system, in: R. Miller, N. Cohen, L. Eriksson, L. Fleisher, J. Wiener-Kronish, W. Young (Eds.), Miller's Anesthesia, Elsevier Saunders, Philadelphia, 2014, pp. 346–386.

[2] R. Freeman, M. Chapleau, Chapter 7 - testing the autonomic nervous system, Editor(s): Gérard Said, Christian Krarup, Handbook of Clinical Neurology 115 (2013) 115–136.

[3] A. Loewy, M. Spyer, Central regulation of autonomic functions, New York, United States: Oxford University Press (1990).

[4] C. Collet, E. Vernet-Maury, G. Delhomme, A. Dittmar, Autonomic nervous system response patterns to basic emotions, Journal of the Autonomic Nervous System 62 (1997) 45–57.

[5] D. C. Fowles, M. Christie, R. Edelberg, W. Grings, D. Lykken, P. Venables, Publication recommendations for electrodermal measurements, The Society for Psychophysiological Research, Inc. 18 (1981) 232–239.

[6] C. Lombardi, M. Pengo, G. Parati, Obstructive sleep apnea syndrome and autonomic dysfunction, Auton Neurosci. 221 (2019) 102563.

[7] M. Kobayashi, N. Tomioka, Y. Ushiyama, T. Ohhashi, Arithmetic calculation, deep inspiration or handgrip exercise-mediated pre-operational active palmar sweating responses in humans, Auton Neurosci. 104 (1) (2003) 58–65.

[8] G. Calcagnini, F. Censi, S. Lino, S. Cerutti, Spontaneous fluctuations of human pupil reflect central autonomic rhythms, Journal of Methods of Information in Medicine 39 (2000) 142–145.

[9] L. Mesin, A. Monaco, R. Cattaneo, Investigation of nonlinear pupil dynamics by recurrence quantification analysis, BioMed Research International 420509 (2013).

[10] L. Mesin, R. Cattaneo, A. Monaco, E. Pasero, Pupillometric study of the dysregulation of the autonomous nervous system by svm networks, Editors: R.J. Howlett, Lakhmi C. Jain, Smart Innovation, Systems and Technologies, Springer (2013) 107–116.

[11] A. Monaco, R. Cattaneo, L. Mesin, I. Ciarrocchi, F. Sgolastra, Dysregulation of the autonomous nervous system in patients with temporomandibular disorder: a pupillometric study, Plos One 7 (9) (2012) e45424.

[12] A. Monaco, R. Cattaneo, L. Mesin, E. Fiorucci, D. Pietropaoli, Evaluation of autonomic nervous system in sleep apnea patients using pupillometry under occlusal stress: a pilot study, Cranio 32 (2) (2014) 139–147.

[13] F. Onorati, L. Mainardi, F. Sirca, V. Russo, R. Barbieri, Nonlinear analysis of pupillary dynamics, Biomedical Engineering / Biomedizinische Technik 61 (1) (2016) 95–106.

[14] A. Venkata Sivakumar, M. Kalburgi-Narayana, M. Kuppusamy, P. Ramaswamy, S. Bachali, Computerized dynamic pupillometry as a screening tool for evaluation of autonomic activity, Neurophysiologie Clinique 50 (5) (2020) 321–329.

[15] S. Aminihajibashi, T. Hagen, M. Foldal, B. Laeng, E. T., Individual differences in resting-state pupil size: Evidence for association between working memory capacity and pupil size variability, Int J Psychophysiol. 140 (2019) 1–7.

[16] S. Jainta, T. Baccino, Analyzing the pupil response due to increased cognitive demand: an independent component analysis study, Int J Psychophysiol. 77 (1) (2010) 1–7.

[17] K. Fröber, F. Pittino, G. Dreisbach, How sequential changes in reward expectation modulate cognitive control: Pupillometry as a tool to monitor dynamic changes in reward expectation, Int J Psychophysiol. 148 (2020) 35–49.

[18] F. Ponzio, A. Villalobos, L. Mesin, C. de'Sperati, S. Roatta, A human-computer interface based on the "voluntary" pupil accommodative response, International Journal of Human Computer Studies 126 (2019) 53–63.

[19] I. Lee, S. Yoon, S. Lee, H. Lee, H. Park, C. Wallraven, Y. Chae, An amplification of feedback from facial muscles strengthened sympathetic activations to emotional facial cues, Auton Neurosci. 179 (1-2) (2013) 37–42.

[20] M. Bradley, L. Miccoli, M. Escrig, P. Lang, The pupil as a measure of emotional arousal and autonomic activation, Psychophysiology 45 (2008) 602–607.

[21] C. Kelbsch, T. Strasser, Y. Chen, B. Feigl, P. Gamlin, R. Kardon, T. Peters, K. Roecklein, S. Steinhauer, E. Szabadi, A. Zele, H. Wilhelm, B. Wilhelm, Standards in pupillography, Front. Neurol. 10 (2019) 129.

[22] M. Strauss, Handwave: Design and manufacture of a wearable wireless skin conductance sensor and housing, Massachusetts Institute of Technology. Department of Mechanical Engineering (2005).

[23] L. de Jesus, J. Rosana, M. Tristao, H. Storm, A. da Rocha, D. Campos, Heart rate, oxygen saturation, and skin conductance: a comparison study of acute pain in brazilian newborns, 33rd Annual International Conference of the IEEE EMBS. Boston, Massachusetts (2011).

[24] D. Li, H. Zhao, S. Dou, A new signal decomposition to estimate breathing rate and heart rate from photoplethysmography signal, Biomedical Signal Processing and Control 19 (2015) 89 – 95.

[25] S. Ghiasi, A. Greco, R. Barbieri, E. Scilingo, G. Valenza, Assessing autonomic function from electrodermal activity and heart rate variability during cold-pressor test and emotional challenge, Sci Rep. 10 (1) (2020) 5406.

[26] K. Khalfallah, H. Ayoub, J. Calvet, X. Neveu, P. Brunswick, S. Griveau, V. Lair, M. Cassir, F. Bedioui, Noninvasive galvanic skin sensor for early diagnosis of sudomotor disfunction: application to diabetes, IEEE Sensors Journal 12 (3) (2012) 456–463.

[27] S. Amplifon, Oculus: Video-oculoscopio digitale, www.biomedica.amplifon.com (2012).

[28] E. Gil, M. Orini, R. Bailón, J. Vergara, L. Mainardi, P. Laguna, Photoplethysmography pulse rate variability as a surrogate measurement of heart rate variability during non-stationary conditions, Physiol. Meas. 31 (2010) 1271–1290.

[29] M. Nitzany, A. Babchenko, B. Khanokhy, D. Landau, The variability of the photoplethysmographic signal- a potential method for the evaluation of the autonomic nervous system, Physiol. Meas. 19 (1998) 93–102.

[30] E. Rodrigues, R. Godina, C. Cabrita, J. Catalao, Experimental low cost reflective type oximeter for wearable health systems, Biomedical Signal Processing and Control 31 (2017) 419–433.

[31] J. Allen, Photoplethysmography and its application in clinical physiological measurement, Physiol Meas. 28 (2007) R1–39.

[32] O. Fathabadi, T. Gale, J. Olivier, P. Dargaville, Automated control of inspired oxygen for preterm infants: What we have and what we need, Biomedical Signal Processing and Control 28 (2016) 9 – 18.

[33] A. Choi, H. Shin, Photoplethysmography sampling frequency: pilot assessment of how low can we go to analyze pulse rate variability with reliability?, Physiol Meas. 38 (2017) 586–600.

[34] M. Dawson, A. Schell, D. Filion, The electrodermal system, Handbook of Psychophysiology. United States: Cambridge University Press (2000).

[35] T. Reinhardt, C. Schmahl, S. Wust, M. Bohus, Salivary cortisol, heart rate, electrodermal activity and subjective stress responses to the mannheim multicomponent stress test (mmst), Psychiatry Res. 198 (1) (2012) 106–111.

[36] M. Benedek, C. Kaernbach, A continuous measure of phasic electrodermal activity, Journal of Neuroscience Methods 190 (2010) 80–91.

[37] B. Figner, R. Murphy, Using skin conductance in judgment and decision making research, in: M. Schulte-Mecklenbeck, A. Kuehberger, R. Ranyard (Eds.), A handbook of process tracing methods for decision research, Psychology Press, New York, 2010.

[38] Atmel, 8-bit avr microcontroller with 16k bytes in-system programmable flash: Atmega16, www.atmel.com (2012).

[39] Atmel, Parametric search of avr microcontrollers, www.atmel.com (2012).

[40] A. Monaco, R. Cattaneo, L. Mesin, E. Ortu, M. Giannoni, D. Pietropaoli, Dysregulation of the descending pain system in temporomandibular disorders revealed by low-frequency sensory transcutaneous electrical nerve stimulation: a pupillometric study, PLoS One 10 (4) (2015) e0122826.

[41] R. Tarjan, Depth-first search and linear graph algorithms, Siam J Comput. 1 (1972) 146–160.

[42] T. Chelimsky, D. Robertson, G. Chelimsky, Disorders of the autonomic nervous system, Daroff: Bradley's Neurology in Clinical Practice. Philadelphia, United States: Saunders Elsevier (2012).

[43] H. Chen, A. Nackley, V. Miller, L. Diatchenko, W. Maixner, Multisystem dysregulation in painful temporomandibular disorders, J Pain 14 (2012) 983–996.

[44] W. Maixner, J. Greenspan, R. Dubner, E. Bair, F. Mulkey, V. Miller, C. Knott, G. Slade, R. Ohrbach, L. Diatchenko, F. R.B., Potential autonomic risk factors for chronic tmd: Descriptive data and empirically identified domains from the oppera case-control study, J Pain 12 (11 Suppl) (2011) T75–T91.

[45] A. Zygmunt, J. Stanczyk, Methods of evaluation of autonomic nervous system function, Arch Med Sci. 6 (2010) 11–18.

[46] K. Kim, S. Bang, S. Kim, Emotion recognition system using short-term monitoring of physiological signals, Med Biol Eng Comput. 42 (3) (2004) 419–427.

[47] R. Fletcher, K. Dobson, M. Goodwin, H. Eydgahi, O. Wilder-Smith, D. Fernholz, Y. Kuboyama, E. Hedman, M. Poh, R. Picard, icalm: wearable sensor and network architecture for wirelessly communicating and logging autonomic activity, IEEE Trans Inf Technol Biomed. 14 (2) (2010) 215–223.

[48] M. Mahmud, H. Fang, H. Wang, An integrated wearable sensor for unobtrusive continuous measurement of autonomic nervous system, IEEE Internet of Things Journal 6 (1) (2019) 1104–1113.

[49] U. Anliker, J. Ward, P. Lukowicz, G. Troster, F. Dolveck, M. Baer, F. Keita, E. Schenker, F. Catarsi, L. Coluccini, A. Belardinelli, D. Shklarski, M. Alon, E. Hirt, R. Schmid, M. Vuskovic, Amon: a wearable multiparameter medical monitoring and alert system, IEEE Trans Inf Technol Biomed. 8 (2004) 415–427.

[50] S. Lee, S. Jung, C. Lee, K. Jeong, G. Cho, S. Yoo, Wearable ecg monitoring system using conductive fabrics and active electrodes, Lecture Notes in Computer Science 5612 (2009) 778–783.

[51] H. Darwish, Wearable and implantable wireless sensor network solutions for healthcare monitoring, Sensors 12 (2012) 12375–12376.

[52] J. Choi, B. Beena Ahmed, R. Gutierrez-Osuna, Development and evaluation of an ambulatory stress monitor based on wearable sensors, IEEE Transactions on Information Technology in Biomedicine 16 (2) (2012) 279–286.

[53] L. Mesin, A neural algorithm for the non-uniform and adaptive sampling of biomedical data, Comput Biol Med. 71 (2016) 223–230.

[54] M. Chen, S. Gonzalez, A. Vasilakos, H. Cao, V. Leung, Body area networks: A survey, Mobile Netw Appl 16 (2011) 171–193.

[55] E. Ortu, D. Pietropaoli, G. Mazzei, R. Cattaneo, M. Giannoni, A. Monaco, Tens effects on salivary stress markers: A pilot study, Int J Immunopathol Pharmacol. 28 (1) (2015) 114–118.

[56] A. Monaco, R. Cattaneo, E. Ortu, M. Constantinescu, D. Pietropaoli, Sensory trigeminal ulf-tens stimulation reduces hrv response to experimentally induced arithmetic stress: A randomized clinical trial, Physiol Behav. 173 (2017) 209–215.

[57] A. Monaco, F. Sgolastra, D. Pietropaoli, M. Giannoni, R. Cattaneo, Comparison between sensory and motor transcutaneous electrical nervous stimulation on electromyographic and kinesiographic activity of patients with temporomandibular disorder: a controlled clinical trial, BMC Musculoskelet Disord. 14 (2013) 168.

[58] J. DeSantana, L. Da Silva, M. De Resende, K. Sluka, Transcutaneous electrical nerve stimulation at both high and low frequencies activates ventrolateral periaqueductal grey to decrease mechanical hyperalgesia in arthritic rats, Neuroscience 163 (4) (2009) 1233–1241.

[59] A. Kalra, M. Urban, K. Sluka, Blockade of opioid receptors in rostral ventral medulla prevents antihyperalgesia produced by transcutaneous electrical nerve stimulation (tens), J Pharmacol Exp Ther. 298 (1) (2001) 257–263.

CONDITIONS	INDEXES with SIGNIFICANT DIFFERENCE
Computation versus **RP (D)**	*Mean HR* (p=0.0002) Comp.: $1.4(1.17, 2.04)$ – RP: 1.08(0.94,1.57) *STD of HR* (p=0.001) Comp.: $0.28(0.17, 0.54)$ – RP: $0.11(0.08, 0.38)$ *STD of GSR* (p=0.0015) Comp.: $1.25(0.54, 2.77)$ – RP: $0.2(0.1, 1.0)$ *Trend of GSR* (p=0.0078) Comp.: $3.03(0.27, 3.28)$ – RP: $-0.12(-1.88, 2.06)$ *Mean pupil area* (p=0.01) Comp.: $6952(6180, 9050)$ – RP: $6565(5839, 8072)$
HDO (D) versus **RP (D)**	*Mean pupil area* (p=0.0029) HDO: $6817(6318, 8636)$ – RP: $6565(5839, 8072)$ *Trend of pupil area* (p=0.012) HDO: $1.05(-0.62, 1.86)$ – RP: $2.10(1.55, 2.63)$ *STD of pupil area* (p=0.024) HDO: $177(142, 279)$ – RP: $267(202,308)$
pre-TENS versus **TENS**	*Mean of pupil area* (p=0.009) pre: $6425(3806, 7391)$ – tens: $5818(3134, 7082)$ *STD of GSR* (p=0.031) pre: $0.11(0.05, 0.27)$ – tens: $0.21(0.72, 0.83)$ *STD of HR* (p=0.036) pre: $0.11(0.07, 0.24)$ – tens: $0.12(0.09, 0.57)$
TENS versus **post-TENS**	*Mean of GSR* (p=0.0001) tens: $12.91(9.09, 14.83)$ – post: $13.65(12.86, 16.61)$
pre-TENS versus **post-TENS**	*Mean of GSR* (p=0.006) pre: $12.88(10.88, 13.68)$ – post: $13.65(12.73, 16.61)$ *Mean area of pupil* (p=0.012) pre: $6425(3806, 7392)$ – post: $5823(3151, 6874)$ *STD of HR* (p=0.022) pre: $0.12(0.08, 0.25)$ – post: $0.16(0.08, 0.35)$
Light versus **Darkness**	*Mean area of pupil* (p<<0.001) L: $2987(2545, 3981)$ – D: $7312(6613, 9059)$ *STD of pupil* (p<<0.001) L: $417(333, 539)$ – D: $220(161, 283)$ *Trend of pupil* (p=0.014) L: $0.23(-0.79, 1.29)$ – D: $1.70(0.21, 2.32)$

Table 2: Statistical analysis of the data using Wilcoxon sign rank test. Mean, standard deviation and trend of data were considered (L: light; D: darkness). Median and quartiles of the indexes showing significant differences ($p<0.05$) are reported (in order of increasing p). Pupil size is indicated in pixels, HR in Hz, GSR in μS; their trends are measured in arbitrary units (they were computed on normalized data and time).